

Snow avalanche hazard and risk assessment in Kullu district, Himachal Pradesh

EXECUTIVE SUMMARY

Authors:

Project Coordinator: Stoffel, M.^{1,2}

Principal Investigator: Ballesteros-Cánovas, J.A.^{1,2}

Co- Principal Investigator: Trappmann, D.¹, Shekhar, M.³, Bhattacharyya, A.³ Bühler Y⁴; Kumar S⁵; Snehmani⁵

1. Institute for Environmental Sciences, University of Geneva, Switzerland

2. DendroLab.ch, University of Bern, Switzerland

3. Birbal Sahni Institute of Palaeobotany, Lucknow, India

4 WSL Institute for Snow and Avalanche Research, Switzerland

5 SASE, India

Study highlights:

- This study combines multidisciplinary approaches to provide a baseline data on snow avalanche event at the upper part of the Beas catchment (Kullu district, Himachal Pradesh) to assess the hazard at transport corridors level between Manali and Lahaul/Spiti.
- More than 51 snow avalanches events for the period 1850–2015 have been reconstructed from disturbances on tree-rings, indicating that snow avalanches activity is a common process in the studied area.
- The combinations of statistical- and spatial- analysis of disturbances allowed identify major events occurred in 1974 and 2006 as well as 4 different snow avalanche activity phases. The baseline data on past snow avalanche activity are linked with climate triggers by mean generalized lineal model (GLM). Results indicate that, rather than precipitation, changes in temperature regimes played and will play an important role in snow avalanche triggering.
- We detected a seasonality shift in the variable correlations from December-January (period 1900-2013) to January-March (period 1950-2013). This shift was consistent taken into account major events (Cluster 3), and may indicate the role of snow-wet avalanche late winter. This findings has important consequence for planning reliable defense structure.
- The application of probabilistic modelling procedures indicates that snow avalanches will reach frequently the transport corridor level. Results indicate the more probable areas to be affected, suggesting the areas where prevention measurement should be focused.
- These results are supported by the numerical model based on accurate topographic data. We have observed the good match between tree-ring dataset and numerical modelling supporting the idea that tree-rings can be used for model calibration

- Based on model, we simulate deposition heights of up to 3 m and pressures higher than 30 kPa at the road level even in the frequent scenario. These results indicate that even frequent avalanches significantly endanger the investigated part of the road.
- Overall, the baseline data created on snow avalanches extends the observations and represents a solid basis for building resilience and reducing snow avalanche risk assessments, by: i) providing the probability of snow avalanche activity at transport corridor level, and ii) underlining the climate triggers related with the larger events and suggesting the potential triggering control of temperatures. The method here describe can be extensively applied to other areas/regions aimed in the baseline data generation useful for adaptation planning.

1. Introduction

Snow avalanches are one of the common slope processes in mountain environments (Luckman, 1977; Eckerstorfer et al., 2013), representing a major threat to corridor infrastructures, insulating and disrupting the status quo of communities and future welfare of those living in those hazard-prone areas. In high mountain domains, snow avalanches processes are affected mainly by climatic factors (e.g. precipitation, temperature, humidity and wind), and terrain factors (e.g. slope, morphometry, aspect, vegetation cover, lithology and earthquakes). The co-occurrence of these factors modifies the snow-pack layer structure in the release zone, its anchorages and internal stability. Under these circumstances, the existence of weak snowpack layer can fail causing that the motion force exceeds the resistance forces and triggering the snow avalanches events which descend along the path until its detection at the bottom of the valley in areas with gentle slope. Triggers mechanism can be, moreover, attributable to localized additional loading caused by humans, animals or large fresh snow, and by abrupt warming (e.g. McClung and Schaerer, 2006). Therefore, the impact of climate change in snow avalanches, and specially the temperature component, is a critical issue (Castebrunet et al., 2014).

The understanding of the natural variability and spatiotemporal patterns of the snow avalanche as well as their trigger mechanisms is essential to design reliable risk reduction strategies and protect critical infrastructures. In this regards, baseline data of past event, and especially those characterized as extreme events, are critical needed to document the chronology and the extent of past avalanches in order to support modelling approaches to determine the hazard zones. Methods used by practioners included the terrain analysis, (e.g., change analysis in time series of aerial photographs, vegetation studies) and/or interviews with (elderly) residents. Nevertheless, these procedures have been showed insufficient to deliver reliable results (Mountan et al., 2009). However, in forested areas, indirect proxies based on tree-ring have been shown as highly reliable

to deliver the past snow-avalanche history. The use of tree rings for the snow avalanche reconstruction has a long history in North America (Potter 1969, Schaerer 1972) and Europe (Corona et al., 2010; Stoffel et al., 2006), and it has become a useful tool to support hazard mapping (Muntán et al., 2009). The main advantages of this methodology are the high spatio-temporal accurate, allowing to date the occurrence of event up to several centuries back. Tree-rings-based snow avalanche chronologies represent, moreover, the unique annual resolved longest-term series to investigate how relationship between climate factor and snow-avalanche events have evolved in the past and determine which impacts due to CC are expecting in the future (Schläppy et al., 2014; 2015).

The objective of this report is to improve our understanding about the spatio-temporal occurrence of past snow avalanches processes in Kullu district, as a basis for hazards assessment and understanding their climate-linkages. The study site is a snow avalanche slope located between Solang and Dhundi villages, which affect recurrently the road given access to the Rothang tunnel. We aims to gather baseline data on snow avalanches based on tree-rings to support future decision-making procedures focused on the road-defense at Solang-to-Dhundi reach. We combine innovative approaches based on tree-ring, statistical modelling and climate analysis to report: i) the longest annual-resolved snow avalanche existing chronology at Indian Himalaya; ii) to investigate the snow avalanche hazard at road-level; iii) to determine the climate-snow avalanche linkages based on the long-reconstructed series.

2. Study area

The study area is located in the western slope reached the road between Solang and Dhundi (upper Beas catchment; coordinates 32.33°-77.14°; Figure 1). This slope is characterized by an unconfined snow avalanche zone with a north-west-orientation and a relief of 4200-2600 masl (1800 m). The accumulation area is characterized by a high gradient spread-forested and homogenous slope, with an average slope around ~35°. The transport zone is partially vegetated by a mixed forest of maple and spruce. The slope here has an average slope around 20°, with a maximum width by almost 1500m. At the level of 2680m, the road accessing to the Rothang Tunnel crosses the entire transport zone in absence of any mitigation/defense infrastructure. This snow avalanche path represents a paradigm about the expected snow avalanche threat in the strategic transport corridor linking Kullu with Lahaul and Spiti.

Geologically, the study snow path is characterized by the Precambrian crystalline schists and gneisses. From climatological point of view, precipitation at the study site is related with the passages of western disturbances related with extratropical pressure system due to: i) low pressure related with upper air cyclonic circulation, and ii) low pressure located on the northern of Pakistan

(Malik, 2012). Methods have been implemented at one study site, although prospective analysis have successfully been done in other snow avalanches areas (Dhundi area), suggesting the capability of replicability of the presented method.

3. Baseline datasets

- Past records of snow avalanche in the nearby areas have been obtained from the available literature (Richardson and Reynolds, 2000; Gardner, 2002; Laxton and Smith, 2009; Malik 2009)
 - Richardson, S. D. and Reynolds, J. M., An overview of glacial hazards in the Himalayas. *Quat. Int.*, 2000, 65, 31–47.
 - Gardner, J., Natural hazard risk in the Kullu district, Himachal Pradesh, India. *Geogr. Rev.*, 2002, 92(2), 282–306.
 - Laxton, S. C., and Smith, D. J., Dendrochronological reconstruction of snow avalanche activity in the Lahul Himalaya, Northern India. *Nat. Hazards.*, 2009, 49(3), 459-467.
 - Malik, A. 2012. Snow avalanche runout modelling in Solang-Dhundi area of Manali, Himachal Pradesh, using a numerical model RAMMS, 2009, PhD. Thesis, National Remote Sensing Center.
 - Bühler et al., 2013. Automated identification of potential snow avalanche release areas based on digital elevation models. *Nat. Hazards Earth Syst. Sci.*, 13, 1321–1335
- Baseline dataset of snow avalanche events has been obtained from dendrogeomorphic interpretation of increment cores samples taken from disturbed trees at the study area.
- Topographic data for probabilistic modelling are based on the ASTER GDEM at 30 m resolution and Lidar resolution (2 to 5 m resolution). Aerial picture of the study site has been obtained from Google Earth.
- No climate station is representative of local climatic conditions due to the remote location of the study site and the lack of access to meteorological data in Kullu. Thus for correlations among climate / snow avalanches, we applied monthly precipitation and temperature data obtained from the Climate Research Unit, GPCC-6, IMD, CRU TS 3.2, 0.5°×0.5°, nearest to the study site. Reanalyzed monthly data set from ERA-interim 1979-"now" and NASA MERRA 1979-"now".

4. Methodology

4.1 Dendrogeomorphic approaches

Due to the lack of available systematic data, in this study the past snow avalanche activity has been inferred from the analysis of growth anomalies of trees growing at the avalanche slope. Classic dendrogeomorphic approaches have been tested and applied at the study site (Stoffel and Corona, 2014). At the field, increment core samples from disturbed trees were obtained by using increment bores. Additional information such as typology of disturbance, geographical location and graphical information were recorded. After sampling preparation, each sample was analyzed following the standard protocols (e.g. Stoffel and Corona, 2014). This protocol involve: i) cross-dating procedures by using point years; ii) growth anomalies identification; and iii) definition of events based on weighted index (Koeling-Mayer et al., 2011). The disturbed trees used as snow avalanche proxies were: i) scars on trees created by the impact of solid material during snow avalanches, ii) tilted trees due to the uni-directional pressure of snow; iii) tree crown lost due to the mechanical impact of the transported debris; iv) survival trees on the snow avalanche track. The growth anomalies related with those disturbed trees were: i) injuries and callus tissues; ii) traumatic resin ducts TRDs; iii) reaction wood; iv) abrupt growth decrease; v) intense growth release. The criteria for event definition have been based on a dynamical-threshold from literature (Corona et al., 2011) involving number of growth disturbance and the weighted index values.

4.2 Probabilistic approaches and modelling

Different statistical and probabilistic approaches have been used to analyses the spatial pattern of the dated events based on the affected tree position. First, in order to distinguish the major events with larger spatial representation in the entire slope of from those minor events characterized with smaller affected areas, a cluster analysis based on k-mean method (Hartigan and Wong, 1979) has been performed on the maximum length and width of the affected areas defined by the affected trees position. Second, probabilistic spatial analyses of snow avalanches have been modeled using a Poisson distribution (Guzzetti, 2000). At each disturbed tree position, a Poisson distribution have been defined based on the tree age and the number of growth disturbance observed in the tree/ring records attributable to snow avalanches. Therefore, the probability (p) for a tree be affected by a snow avalanche with a return period (T) to occur in a given number of years N (e.g. fixed to 5, 10, 20, and 100 years) can be computed as follow (Eq.1):

$$p = 1 - e^{\left(-\frac{N}{T}\right)}$$

This statistic model has been widely used for describing natural hazards under the assumption (Guzzetti et al., 2005; Lopez-Sáez et al., 2012): (i) the snow avalanche events are independent; (ii) the probability of an event occurring in a very short time is proportional to the time interval, and negligible if an event took place in a short time interval (iv) the probability distribution of the number of events is the same for all time interval, consequently the mean recurrence of events will remain the same in the future as it was observed in the past.

4.3 Numerical simulation

Numerical simulations rapid mass movements such as snow avalanches, debris flows or rockfalls are important tools for hazard mapping and mitigation measure planning (Christen et al., 2012). We apply the Voellmy-Salm modeling approach (Voellmy, 1955) implemented in RAMMS:AVALANCHE developed at the WSL Institute for Snow and Avalanche Research SLF (Christen et al., 2010), to simulate different hazard scenarios in a catchment along the Solang road.

Due to the limited information, we are in need for an automated avalanche release identification tool. Such a tool was developed and tested by (Bühler et al., 2013). A further development of this tool, taking into account also the smoothing of the terrain by snow and the dominating wind direction is developed by (Veitinger et al., 2015). We use this approach (Fig 2.) to identify potential avalanche release zones for a test-catchment along the Solang road. We choose a release probability limit of 65% to generate the potential release polygons and edited them manually based on slope angles and terrain homogeneity (Fig 3.). We used Lidar data 5x5m as input topographic data.

To simulate an extreme (i.e. > 300 years return period), an intermediate (i.e. ~ 100 years return period) and a frequent (i.e. ~ 10 years return period) avalanche event we simulated a starting off all release zones together. This is not what happens in reality but gives us a good picture of the area potentially affected by avalanches for a given scenario. For a detailed hazard analysis every release zone would have to be simulated for it self and adapted to the scenario by changing its size. For this preliminary investigation we did not change the size of the release zones but we vary the release depth and the friction parameters for every scenario according to Table 1.

Table 1. Model parametrization for each scenario considered.

| Scenario | Extreme | Intermediate | Frequent |
|--------------------------|-------------|--------------|-------------|
| Average release depth | 1.5 m | 1 m | 0.5 m |
| Coulomb friction μ | 0.16 – 0.27 | 0.2 – 0.33 | 0.22 – 0.35 |
| Turbulent friction ξ | 1500 – 3000 | 1350 - 2500 | 1200 – 2000 |

4.4 Snow avalanche-climate linkages

Two different analyses have been performed in order to describe the relationship between climate and snow avalanche events. First, due to the lack of availability of direct data on precipitation, snowfall, wind and temperature at Dhundi area, gridded data from Climate Research Unit, GPCC-6, IMD and CRU TS 3.2 have been used to describe monthly anomalies, defined relative to the reference period 1980-2010 according with the Eq.2, in: i) monthly precipitation, ii) accumulated precipitation, iii) maximum, mean and minimum surface temperature, iv) wind intensity, as well as v) interaction between precipitation and temperature. Grid snowpack data and wind were not taken into account due to the low resolution of this dataset. Initially, a PCA (Principal Component Analysis) has been performing in order to distinguish autocorrelation between the input climate variables (e.g. reduce the analysis dimension).

$$X_{ji}^{\text{ref}}(t) = \frac{X_{ij} - \mu_{\text{ref}}}{\sigma_{\text{ref}}}$$

where μ_{ref} and σ_{ref} are the mean and standard deviation for the reference period and x_{ij} the value for each specific month, respectively.

Based on this dataset, generalized linear models (GLMs) have been used to investigate the relationship between the dichotomous response variable, i.e., the occurrence or non-occurrence of avalanche events in year t , and climatic explanatory set variables.

$\text{logit}(p_t) = \beta_0 + \beta_1 x_{ij} + \dots + \beta_k x_{kt}$, being p_i the probability to have a snow avalanche, β_0 the intercept, β_i regression coefficients and x_{kt} climate variables. The binomial link function is the $\text{logit}(p_t) = \ln(p_i/1 - p_i)$.

Due to the large number of variables initially considered, we first apply a correlation analysis to reduce the dimension of covariates. Then, we built full models for each uncorrelated family of variables and apply standard selection procedures (SSP) based on the Akaike Information Criterion (AICc, Burnham and Anderson 2002), which combine a measure of goodness of fit with a penalty term based on the number of parameters (k) used in the model. In order to identify potential changes in the climate-event linkage, this procedure was applied for the periods: i) 1900-2013, and ii) 1950-2013. We also tested the hypothesis related with those major snow avalanche event identified by cluster analysis on the geographical extension of snow avalanches. The criteria to select suitable models was: i) insolate variables from the full model (initial model including all covariate) with large impact in AIC index (difference + 2 units); ii) based on those variables

initially insolated, built model with much lower AIC values (> 4 units) than the null model (model without considering any variables).

5. Results

5.1 Baseline data reconstruction on snow avalanches

- The analysis of more than 250 samples from 144 disturbed trees due to past snow avalanches has allowed to reconstruct 51 past events since 1855, defining an average frequency of 0.32 events year⁻¹ (Figure1). Overall, forty-one events can be considered as undouble events (satisfice threshold: #GD >5 and Wit >0.75), whereas ten cases may be considered as “potential events” (satisfice threshold: #GD=4 and $0.5 < \text{Wit} < 0.75$).
- For the reference studied period (since 1980-to-present); our data point out an occurrence of snow avalanches events by almost 0.63 events year⁻¹ (22 snow avalanches events). These findings underline the current snow avalanche hazard at the study area and may reflect the state of nearby slopes in the upper Beas catchment.
- At long-term, our reconstruction shows the existence of snow-avalanche inactivity between 1940-60’s; and two different phases since 70’s, with almost annual events from 1989 to 2003 and high frequency (0.875 events year⁻¹) between 1970 and 1977; and a decrease in the frequency from 1977 to 1989 and 2003 to present.
- According with our baseline dataset, the largest snow avalanche event took place in 1973/74, affecting the entire studied slope and the road level. Extreme snow avalanche events took place as well in 1978/79, 1982/83 and recently in 2005/06 (Figure 2). Based on the K-means algorithm (cluster analysis of the affected area), at least 23 events were categorized as “larger events”, with a related average affected width of $693 \pm 89\text{m}$. (Figure 3).

5.2 Snow avalanche hazard assessment

- The spatial analyses of the snow avalanche reconstruction highlights the current snow-avalanche hazard at road level and evidence the needed to carry out protective measurement

in order to maximize its future utility. Therefore, based on the baseline data on past snow avalanche frequency, the reliability of the Rothang tunnel may be related with the future capacity to defense against snow avalanches events the entire road from Solang village.

- The statistical modelling suggests that the current hazard at the entire studied reach transport corridor is noteworthy. For a return period corresponding to $T=10$ yrs., the probability of the road to be affected by snow avalanche increase up to 0.54. Considering return periods of $T=25$ yrs., the probability may even increase up to 0.80. The expected affected road area by snow avalanche increase considerably when return periods of $T=50$ and $T=100$ yrs. are considered, with probabilities close to 0.90.
- The simulation results of the extreme scenario (300y) show that nearly the entire area of interest can be affected by extreme avalanche events (Fig 6a.) The highest flow velocities confine the main flow paths. In the 100 year intermediate scenario larger parts in particular along ridges are not affected by the flowing part of the simulated avalanches (Fig 6b). In the frequent scenario only the main gullies are affected (Fig 6c). However even the avalanches in the small scenario overflow the road and reach the river in the valley bottom. We simulate deposition heights of up to 3 m and pressures higher than 30 kPa at the road even in the frequent scenario. The Figure 7 shows an example of model results from RAMMS and tree position related with the 2006 events. In this example, the good match between field observation and modelling indicate that tree-ring can be used for model calibration, and consequently to improve hazard and risk assessment. These results indicate that even frequent avalanches significantly endanger the investigated part of the road.
- This result, together existing observation in nearby areas, clearly point out that building resilience will be based on proper defence strategies at road level in order to avoid the disruption of transport infrastructures.

5.3 Snow avalanche-climate relationships

- The reconstructed snow avalanche activity has allowed investigating the main climatic control on triggering. Due to the lack of available systematic climate data for this study, we

have used a limited number of gridded dataset at monthly scale variables related with precipitation, wind and temperature anomalies.

- The GLM suggest that triggering snow avalanche at the studied site during last century was mostly related with the precipitation and maximum anomalies in March. This was especially clear for the period between 1970-2013, and for those major snow avalanche events categorized as “cluster 3”. Tested model are showed in Table 1. From AIC analysis, robust model reported a difference between AIC H_{null} and AIC_{model} ranked -7.9 and -2.2. In general, model related with the T_{min} covariate were more robust than those obtained with the T_{max} covariate.
- Analysing T_{min} covariate, results indicate that taken into account all reconstructed event since 1900, the occurrence of events are related with (+) anomalies of T_{min}D, T_{min}J, and interaction between T_{min}M and P_{acu}M. Analysing T_{max} covariate, results indicate that events were related with (+) anomalies of T_{max}D, T_{max}J, T_{max}F, and (-) anomalies T_{max}D.
- Taken into account the larger snow avalanches (cluster 3), the variable influenced the occurrence of snow avalanche experimented a seasonal shift between the period 1900-2013, and those took place between 1950-2013. Since 1900, the snow avalanche were related with (+) anomalies of T_{min}D, T_{min}J, and T_{min}J: P_{acu}J; whereas since 1950, the snow avalanche were related with (+) anomalies of T_{min}J and T_{min}M: P_{acu}M.

6. Discussion of results

Our study provides a robust and the longest spatio-temporal baseline dataset for dealing with adaptation to snow avalanche hazards under CC in Kullu district. This study has addressed three different framework components: i) Hydrometeorological event, ii) Exposure analysis; and iii) Climate Change and natural variability. Rather than large scale analysis, based on not well-resolved geographical and thematic models and highly fragmented or inexistent historical records, this study has been focused on reconstructing at annual level the longest snow avalanche activity in a paradigmatic snow avalanche path, which will be critical for the future reliability of the strategic transport corridor between Kullu and Spiti; and, consequently, improve the resilience of inhabitants. The gathered snow avalanche data set has demonstrated that the snow avalanche activity at the study site is noteworthy, with periods characterized by annual events, highlighting the probability of the road to be damage as well as the climate-event linkages.

The amount information related with snow cover and historical records of snow avalanche available to validate this study was limited. Based on Malik (2012), we found that in the nearby area snow avalanches took place in 2003, 2004, 2005 and 2006. Several snow avalanche events (up to 4) took place 2005. In five cases, snow avalanche were in March, whereas in three case were in February and one case in January. All those years were found in our dataset and therefore are supporting our findings about the high frequency as well as the potential seasonality of snow avalanche events in recent years. The long-term chronology as well as the event definition threshold is based on a tested methodology (p.e. Corona et al., 2012). We used an adaptive threshold to maximize the information recorded in the tree-rings (Chiroiu et al., 2015).

Our methodology has revealed a large snow avalanche activity, pointed out an average frequency by almost $0.32 \text{ events year}^{-1}$ (considering the dataset since 1855) and $0.59 \text{ events year}^{-1}$ (considering the dataset since 1950). This frequency is higher than those observed in the Glacier National Park in USA ($\sim 0.28 \text{ events year}^{-1}$; Pederson et al., 2006); French Alp ($\sim 0.2 \text{ events year}^{-1}$; Corona et al., 2010); in Carpathians Mountains ($\sim 0.13 \text{ events year}^{-1}$; Chiroiu et al., 2015); in Spanish Pyrenees ($\sim 0.9 \text{ events year}^{-1}$; Muntan et al., 2004); and therefore, contextualize at global scale the extraordinary frequency of snow avalanche in Kullu district. Our reconstructions have also showed the existence of dissimilar snow-avalanche activity phases during last century. We detected lower snow avalanche activity between 1940-60's; 1977 – 1989; and 2003 to present; whereas higher activities were clearly detected between 1970-1977 and 1989-2003.

The lack of available accurate topographic information avoided the use of numerical simulation, required for spatial pattern analyses. However, our stochastic approach has been showed as useful to identify the affected area at road level and their expected probabilities. Large probabilities of snow avalanche occurrence are therefore expected at road level, highlighting the needed to protect the road infrastructure to improve resilience in future scenarios. Therefore, transport corridor disruption may result in a more vulnerability state of affected service. Taken into account that large investment in renewal the transport corridor frequently affected by snow avalanche may limit the

opportunity to invest resources in other sensible areas, the proper defence of this infrastructure will be critical to improve its reliability at long-term.

We used GLM to investigate the relationship between snow avalanche activity and climate variables. We successfully tested the hypothesis if there were a shift in the climate-related triggers at long and shorter term. In this study, we did not checked relationship between annual resolved snow and climate variables, as it has been demonstrated less efficiency than monthly variables (Schlappy et al., 2015). Our results indicate that the occurrences of snow avalanche were related with monthly temperature regime anomalies, rather than precipitation (only appear to be interesting when interact with temperature) or wind. The most interesting findings were that for those large events categorized with the cluster 3, we observed a seasonal shift in the explicative variables from December, January, if we consider the period 1900-2013, to January, March, if we consider the period since 1950. This shift may suggest a more dense snow avalanche, categorized with a significant increase of the minimum and maximum average temperature, which it may have an important role in the design of defence strategies. Given that temperatures and precipitation regime are expected to increase in Indian Himalayas (Bhutiyan et al., 2007); the hypothesis that more dense snow avalanche in late winter cannot be rejected based on the gathering baseline dataset here reported.

7. Work in progress

The Swiss-Indo join collaboration partner will finalize the analysis of climate factors related with extreme events and the final interpretation and discussion of results. The Swiss partner will continue the snow avalanche analysis by coupling numerical modelling into statistical approaches. It is expected to provide Stochastic Life cycle assessment to compile all the information here reported and highlight the importance of defence strategies.

8. Perspectives for upscaling

- The outcome of the study will help in addressing various issues related to snow avalanche risks, hazards and climate change, as incorporate both temporal and spatial dimension. The idea to improve the reliability in corridor infrastructure as a key driver to improve resilience (improve services and markets) in remote mountain areas during the entire year.
- Methodology is robust, as it has been previously applied in several mountain ranges worldwide.
- Due to the ubiquity of trees in the Himalayas slopes, the methodology here reported are useful for upscaling the procedure in other regions, as they have been showed consistent with those obtained in other sites.
- It is needed more specific studies to develop indexes based on geomorphology and morphometric to up-scale potentiality of a zone to snow-avalanches, but the climate-relationship here found can help to improve our understanding for other geomorphological-delineated snow-avalanches areas.

References

- Bühler, Y., Kumar, S., Veitinger, J., Christen, M., Stoffel, A. and Snehmani, 2013. Automated identification of potential snow avalanche release areas based on digital elevation models. *Natural Hazards and Earth System Science*, 13(5): 1321-1335.
- Bhutiyani, M.R., Kale, V.S. and Pawar, N.J., 2007. Long-term Trends in Maximum, Minimum and Mean Annual Air Temperatures across the Northwestern Himalaya during the Twentieth Century. *Climatic Change* 85, 159-177.
- Chiroiu, P., Stoffel, M., Onaca A., Urdea, P. (2015): Testing dendrogeomorphic approaches and thresholds to reconstruct snow avalanche activity in the Fagara? Mountains (Romanian Carpathians). *Quaternary Geochronology* 27, 1–10.
- Christen, M., Bühler, Y., Bartelt, P.a.L., R.and Glover J, Schweizer, A.a.G., C, McArdell, B.W., Gerber, W., Deubelbeiss, Y., Feistl, T. and Volkwein, A., 2012. Integral hazard management using a unified software environment: numerical simulation tool "RAMMS" for gravitational natural hazards. In: G. Koboltschnig, J. Hübl and J. Braun (Editors), *Interpraevent*, pp. 77 - 86.
- Christen, M., Kowalski, J. and Bartelt, P., 2010. RAMMS: Numerical simulation of dense snow avalanches in three-dimensional terrain. *Cold Regions Science and Technology*, 63: 1 - 14.
- Corona, C., Lopez Saez, J., Stoffel, M., Bonnefoy, M., Richard, D., Astrade, L., Berger, F. (2012): How much of the real avalanche activity can be captured with tree rings? An evaluation of classic dendrogeomorphic approaches and comparison with historical archives. *Cold Regions Science and Technology* 74–75: 31–42
- Corona, C., Rovéra, G., Lopez Saez, J., Stoffel, M., Perfettini, P. (2010): Spatio-temporal reconstruction of snow avalanche activity using tree rings: Jean Jeanne avalanche talus, Massif de l'Oisans, France. *Catena* 83:107–118
- Eckerstorfer, M., Farnsworth, W.R., Birkeland, K.W., 2013. Potential dry slab avalanche trigger zones on wind-affected slopes in central Svalbard. *Cold Regions Sci. Technol.* 99, 66e77.
- Gardner, J., Natural hazard risk in the Kullu district, Himachal Pradesh, India. *Geogr. Rev.*, 2002, 92(2), 282–306.
- Guzzetti, F., Reichenbach, P., Cardinali, M., Galli, M., Ardizzone, F., 2005. Probabilistic landslide hazard assessment at the basin scale. *Geomorphology* 72, 272–299.
- Hartigan, J. A., & Wong, M. A. (1979). Algorithm AS 136: A k-means clustering algorithm. *Applied statistics*, 100-108.
- Laxton, S. C., and Smith, D. J., Dendrochronological reconstruction of snow avalanche activity in the Lahul Himalaya, Northern India. *Nat. Hazards.*, 2009, 49(3), 459-467.
- Lopez Saez, J., Corona, C., Stoffel, M., Schoeneich, P., Berger, F. (2012): Probability maps of landslide reactivation derived from tree-ring records: Pra Bellon landslide, southern French Alps. *Geomorphology*.

- Luckman, B.H., 1977. The geomorphic activity of snow avalanches. *Geogr. Ann.* 59A (1e2), 31e48
- Malik, A. Snow avalanche runout modelling in Solang-Dhundi area of Manali, Himachal Pradesh, using a numerical model RAMMS, 2009, PhD. Thesis, National Remote Sensing Center.
- Muntan, E., Garcia, C., Oller, P., Martí, A., Garcia, A., Gutiérrez, E., 2009. Reconstructing snow avalanches in the Southeastern Pyrenees. *Natural Hazards and Earth System Sciences* 9, 1599–1612
- Richardson, S. D. and Reynolds, J. M., An overview of glacial hazards in the Himalayas. *Quat. Int.*, 2000, 65, 31–47.
- Schläppy, R., Jomelli, V., Eckert, N., Stoffel, M., Grancher, D., Brunstein, D., Corona, C., Deschatres, M. (in press): Can we infer avalanche?climate relations using tree-ring data? Case studies from the French Alps. *Regional Environmental Change*.
- Schläppy, R., Eckert, N., Jomelli, R. Stoffel, M., Grancher, D., Brunstein, D., Naaim, M., Deschatres, M. (2014): Validation of extreme snow avalanches and related return periods derived from a statistical-dynamical model using tree-ring based techniques. *Cold Regions Science and Technology* 99, 12–26.
- Stoffel, M., Corona, C. (2014): Dendroecological dating of geomorphic disturbance in trees. *Tree-Ring Research* 70, 3–20.
- Veitinger, J., Purves, R.S. and Sovilla, B., 2015. Potential slab avalanche release area identification from estimated winter terrain: A multi-scale, fuzzy logic approach. *Nat. Hazards Earth Syst. Sci. Discuss.*
- Voellmy, A., 1955. Über die Zerstörungskraft von Lawinen. *Schweizer Bauzeitung*, 73: 159 - 285

FIGURES:

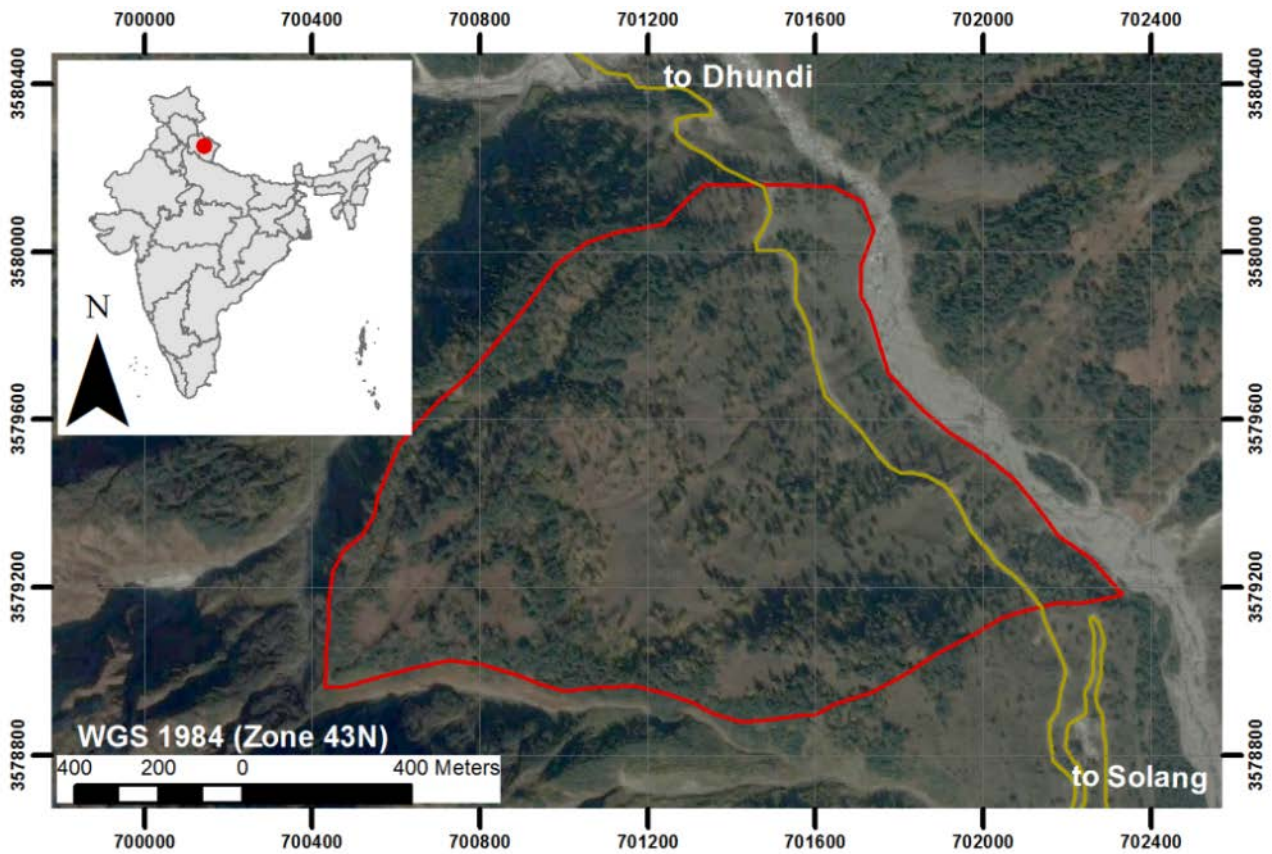


Figure 1: Analyzed snow avalanche paths located between Solang and Dhundi (Kullu district, Himachal Pradesh).

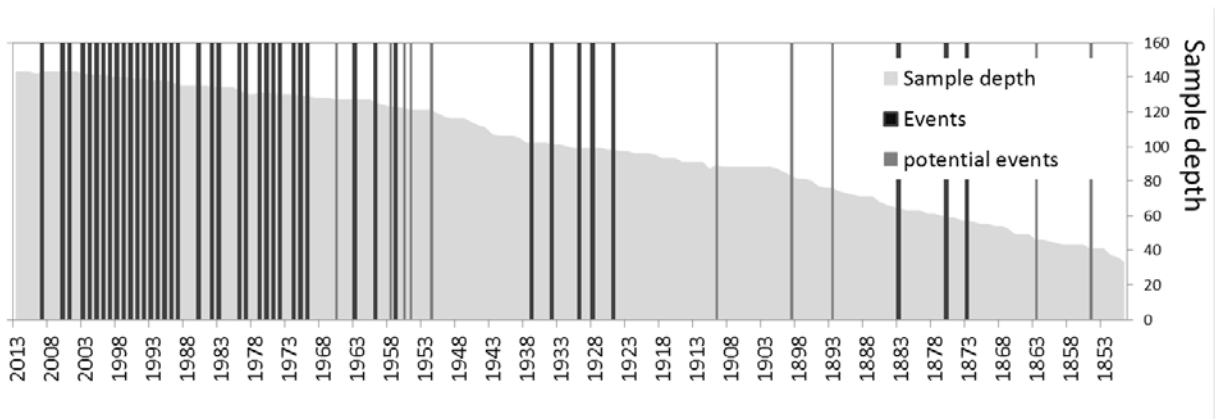


Figure 2: Snow-avalanche reconstruction. Used thresholds for dating snow avalanche events: i) event, $n^{\circ}GD > 5$ and $Wit > 0.75$; ii) potential events, $\#GD > 4$ and $Wit > 0.5$.

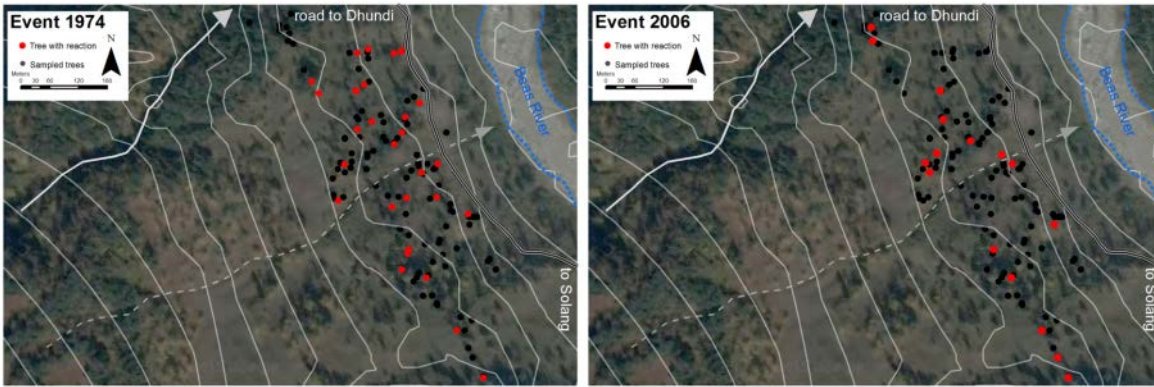


Figure 3. Examples of spatial snow avalanche pattern for the large events took place in 1974 and 2006. Affected trees were located close to the road level and along the entire studied slope.

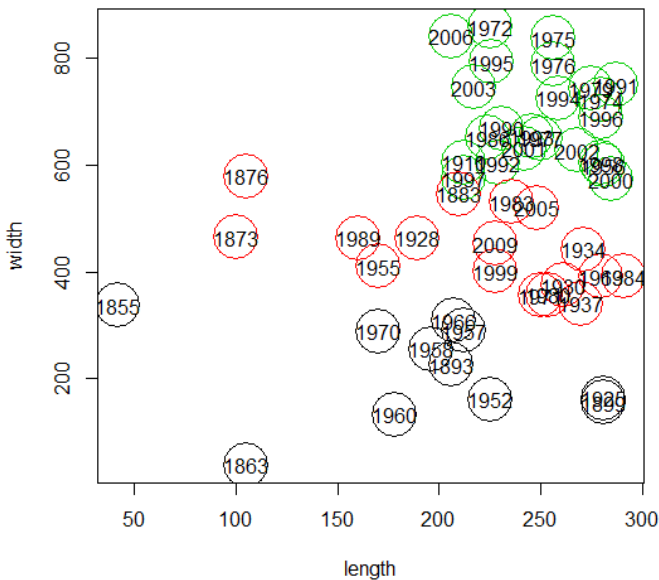


Figure 4. Cluster analysis based on the reconstructed extension of the past snow avalanche events took place at the study site since 1850. Cluster 3 (on green) represents the years where massive affecting the entire slope and reaching the road level events took place; Cluster 2 (on red) represents moderate events; Cluster 1 (on black) represents narrower (more channelized) events.

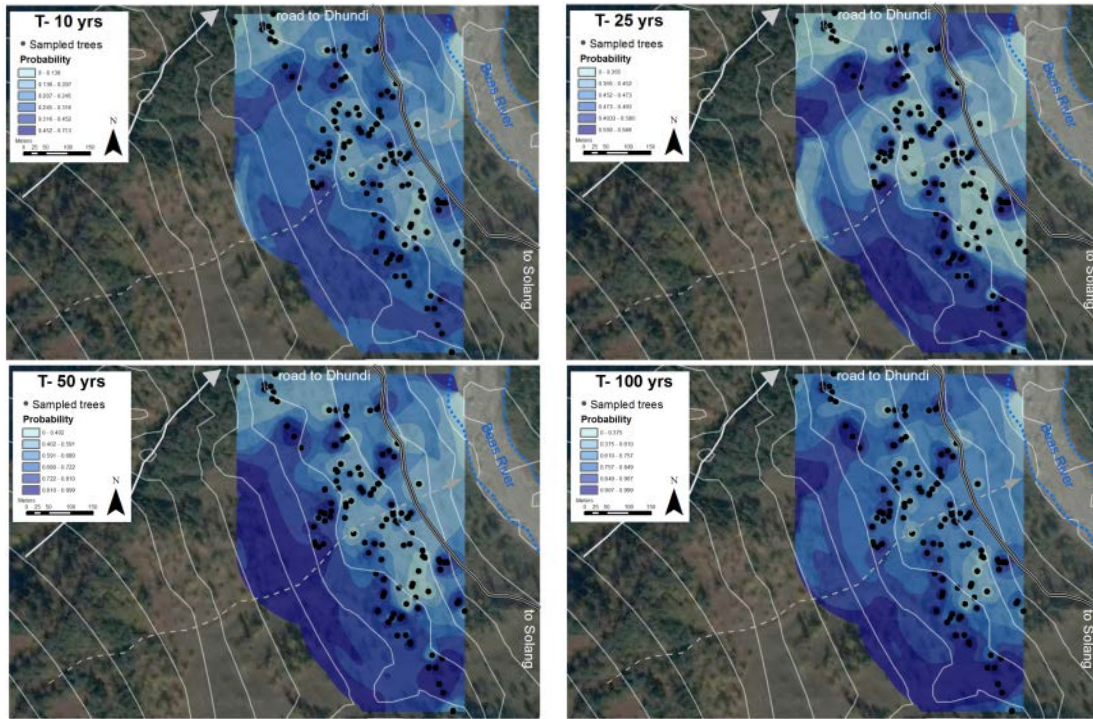
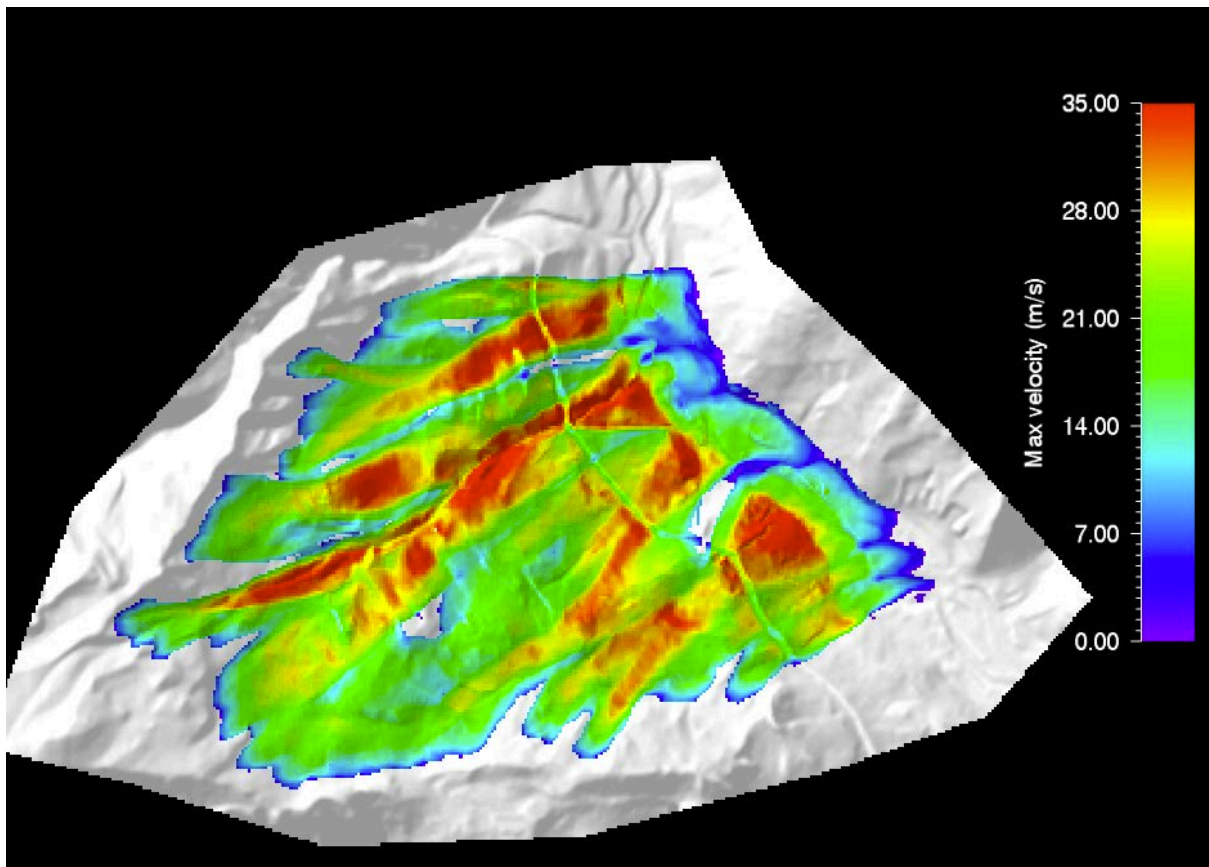


Figure 5. Probabilistic map (T=10, 25, 50 and 100 years) showing the probability one tree be impacted by snow-avalanches at the studied slope.



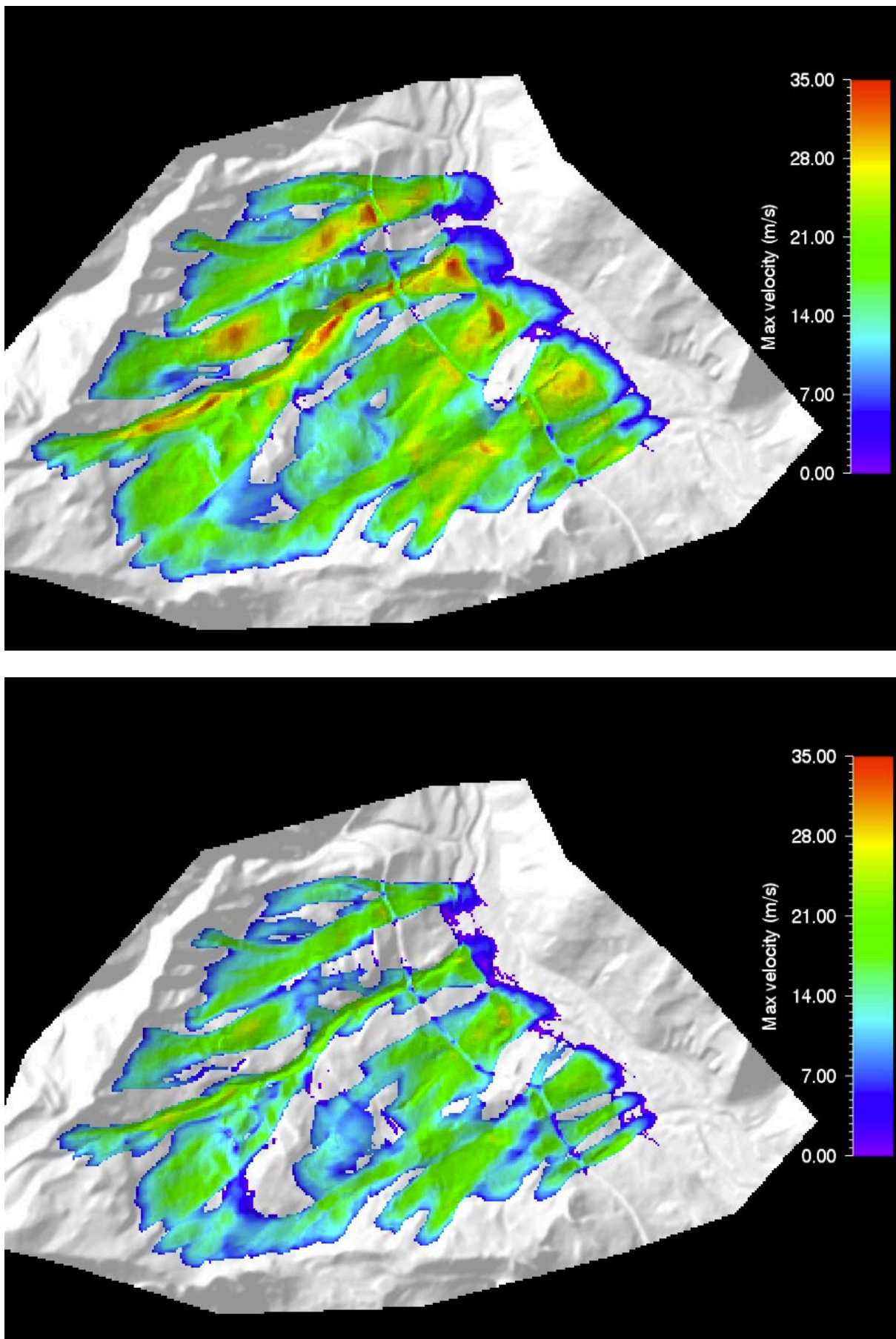


Figure 6. Simulated maximum velocities of the extreme scenario (300y top), the intermediate scenario (100y middle) and the frequent scenario (10y bottom)

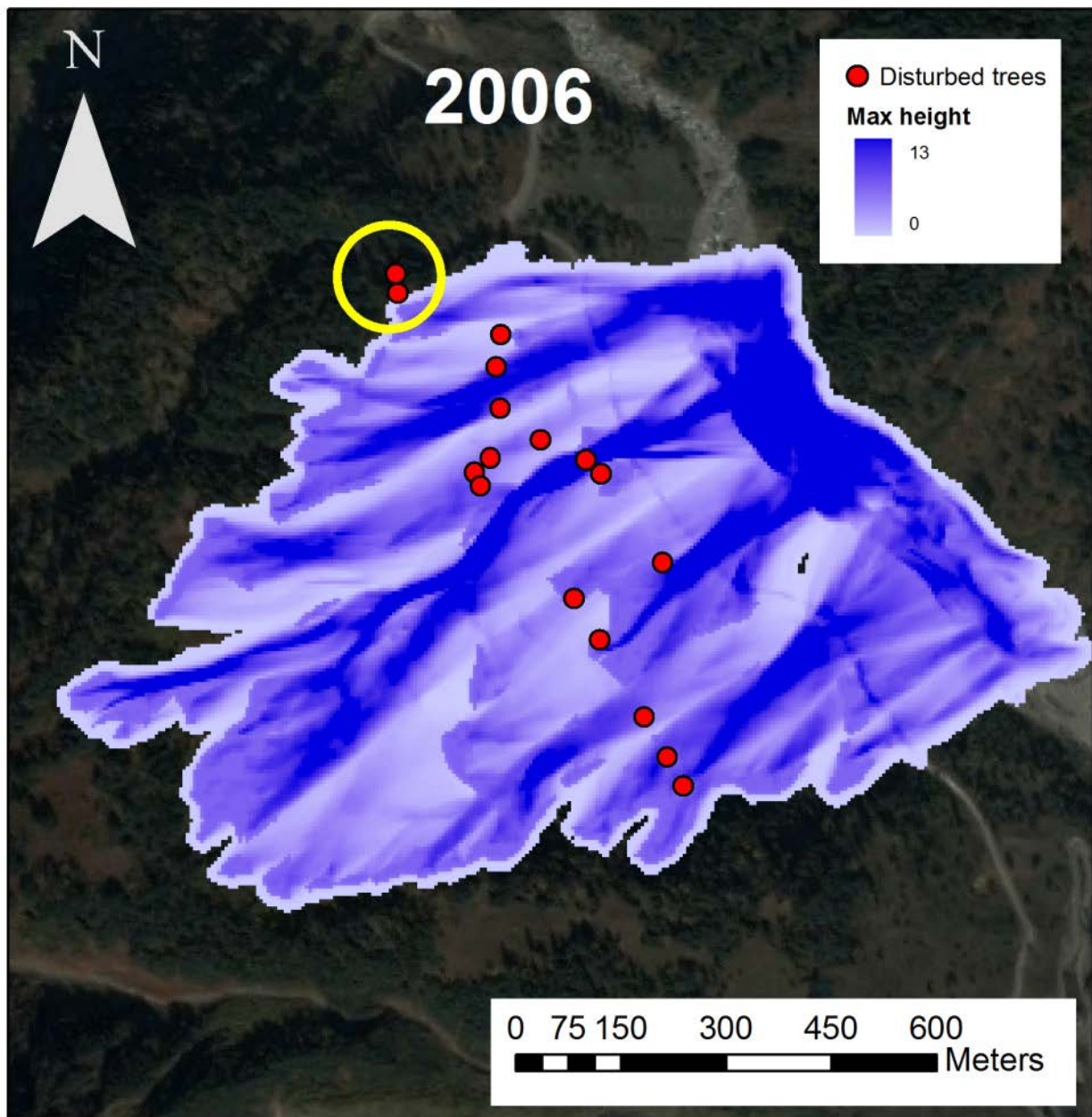


Figure 7. Match between disturbed trees during the 2006 snow avalanche and the modelled maximum height for the intermediate modelling scenario (T=100 years). The yellow circle indicates an example of unmatched between tree position and model results, suggesting those trees may be affected by events on the left corridor.

Table 2. Parameter results from the best generalized lineal model obtained by applying the SSP from the full model, taking into account all events and events categorized as cluster 3 during the period 1900-2013 and 1950-2013. Larger difference between AIC model and AIC null (> -2) suggest robust model. Best models are indicated with (*) (lower AIC values).

| | | Intercept (Estimate Std. Error) | variable #1 (Estimate Std. Error) | variable #2 (Estimate Std. Error) | variable #3 (Estimate Std. Error) | Variable #4 (Estimate Std. Error) | AIC _{model} | AIC _{H_{null}} | Diff. AIC |
|-------|--|---------------------------------------|---|---|---|---|----------------------|---------------------------------|-----------------|
| T min | (*) Event ₁₉₀₀ ~ T_min_D+T_min_J+T_min_M:P_acu_M | 0.09778 0.24836 | 0.39050 0.21654 | 0.56022 0.23950 | 0.63710 0.36784 | | 142.56 | 150.0626 | -7.5026 |
| | Event ₁₉₅₀ ~ T_min_M+T_min_M:P_acu_M | 0.4635 0.2745 | -0.3480 0.2974 | 0.7336 0.5822 | | | 89.669 | 88.45947 | 1.20953 |
| | (*) Event _{1900_cluster3} ~ T_min_D+T_min_J+T_min_J:P_acu_J | -0.6423 0.2766 | 0.4502 0.2552 | 0.5816 0.2943 | 0.8660 0.4963 | | 95.78 | 103.7101 | -7.9301 |
| | (*) Event _{1950_cluster3} ~ T_min_J+ T_min_M:P_acu_M | 0.1457 0.3365 | 0.8026 0.3731 | 1.0309 0.6476 | | | 65.7833 | 68.20841 | -2.42511 |
| Tmax | Event ₁₉₀₀ ~ T_max_D+T_max_J+T_max_F+T_max_M | -0.1616 0.2179 | 0.3267 0.2254 | 0.2479 0.2362 | 0.4266 0.2096 | -0.1195 0.2431 | 147.86 | 150.0626 | -2.2026 |
| | (*) Event ₁₉₅₀ ~ T_max_J+T_max_M | 0.4315 0.2666 | 0.4886 0.3127 | -0.4438 0.3004 | | | 88.06 | 88.45947 | -0.39947 |
| | Event _{1900_cluster3} ~ T_max_J+T_max_J:P_acu_J | -0.9363 0.2507 | 0.2728 0.2736 | 0.7869 0.4440 | | | 102.02 | 103.7101 | -1.6901 |
| | Event _{1950_cluster3} ~ T_max_J+T_max_M+P_acu_M+WIND_D | 1.1663 0.7227 | 0.6457 0.3683 | -0.9280 0.4259 | -0.8187 0.6807 | -3.4944 1.8703 | 66.954 | 68.20841 | -1.25441 |